Available online at www.sciencedirect.com
SCIENCE DIRECT
Journal of Photochemistry and Photobiology A: Chemistry 176 (2005) 50–67
Journal of Photochemistry and Photobiology A:Chemistry
www.elsevier.com/locate/jphotochem

Spectroscopic studies of the I_2/O_3 photochemistry Part 2. Improved spectra of iodine oxides and analysis of the IO absorption spectrum

Peter Spietz *, Juan Carlos Gómez Martín, John P. Burrows

Institute of Environmental Physics (IUP), University of Bremen, Otto Hahn Allee 1, PO Box 330440, 28334 Bremen, Germany

Received 15 July 2005; received in revised form 12 August 2005; accepted 12 August 2005
Available online 26 September 2005

Abstract

Based on multivariate statistical separation techniques spectra of iodine oxides formed in the photolysis of $I_2 + O_3$ have been obtained. Data was recorded by time resolved UV–vis absorption spectroscopy. Overlapped spectra of ground state IO($\nu' \leftarrow 0$), vibrationally excited IO($\nu' \leftarrow \nu''$) with $\nu'' > 0$, and OIO have been separated from each other and from underlying absorptions of further iodine oxides. The uncertainty due to uncorrected foreign absorptions is of no more than ±3%. Relative errors of spectra are of the order of a few percent for the main parts of the spectra. The up to now unknown continuous parts of spectra are thereby determined. Previous uncertainties in differential absolute absorption cross-section are removed. By the separation of the ground state IO spectrum from that of vibrationally excited IO spectroscopic measurements under non-equilibrium conditions are enabled. Three further absorber spectra have been extracted in the 200–600 nm window. Two of them are most likely caused by I_2O_2 and possibly I_2O_3 thereby providing part of the missing link between IO and OIO consumption and the formation of higher oxides and possibly aerosol. All spectra are available as supplementary data.

Given the unprecedented quality of extracted spectra for the first time an analysis of band strength of the IO($A^2\Pi_{3/2} \leftarrow X^2\Pi_{3/2}$) transition could be made. The continuum absorption of the ground state IO spectrum was resolved into overlapped bands of bound–bound transitions and two bound-free transitions. From the bound-free transitions found the existence of two optically active repulsive states intersecting with the IO($A^2\Pi_{3/2}$) potential has been inferred and tangents to the two repulsive potentials have been determined. Correlating the tangents to probable dissociation products gives a plausible rough picture of the shape of the repulsive states which is in good agreement with previous observations on predissociation of states. There is evidence that one of the continuous absorptions observed could have its origin in the IO($^2\Pi_{1/2}$) sub-system. Relative band strength was determined for absorption bands of IO($A^2\Pi_{3/2} \leftarrow X^2\Pi_{3/2}$). They are in good agreement with literature and with simple calculations based on a Morse approximation. An anomalous behaviour of IO($2 \leftarrow 0$) in time resolved measurements was observed and studied. It could be explained by a hypothetical partial population inversion of the IO($A^2\Pi_{3/2}$) state, but the source of it remains unclear.

Keywords: Iodine oxides; IO; OIO; Absorption cross-section spectra; Vibrationally excited IO; IO potentials; Franck–Condon factors

1. Introduction

Gas phase UV–vis spectra of iodine oxides appeared quite frequently in past publications. While many publications on iodine oxides were focussed on studies of chemical kinetics and on determination of single wavelength absolute absorption cross-sections e.g. [1–9], the observation of spectra was reported rather as a by-product. Interestingly those publications concentrating on spectra as such and on spectroscopic analysis – dominantly IO and later OIO – are some of the earliest [10,11] and then only among the more recent ones e.g. [12,14–17]. In general the formation of higher iodine oxides – other than IO and OIO – is out of question. This is, because in all experiments usually the amount of iodine originally released to form IO and OIO is returned only at a fraction as I or I_2, once IO and OIO are consumed. But references to spectra of possible products – if observed at all – are scarce [18,6,9].

The publications reporting absorption or emission spectra can be divided into two groups. Firstly those reporting more or less complete band systems of UV–vis electronic spectra

* Corresponding author. Tel.: +49 421 218 4585; fax: +49 421 218 4555.
E-mail address: peterspietz@iup.physik.uni-bremen.de (P. Spietz).

1010-6030/$ – see front matter © 2005 Elsevier B.V. All rights reserved.
doi:10.1016/j.jphotochem.2005.08.023

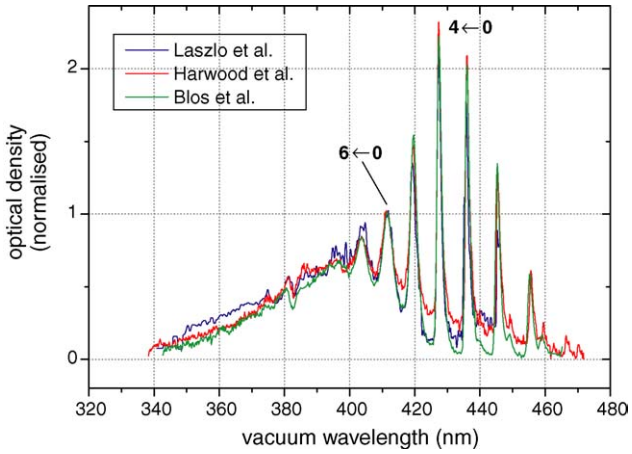

Fig. 1. For IO a number of previously published spectra exist. For comparison they have been scaled to the broad (6 ← 0) absorption band. They all show different amounts of uncorrected background absorptions and fail to determine the ends of the spectrum clearly. There is also disagreement with respect to the height of the bands.

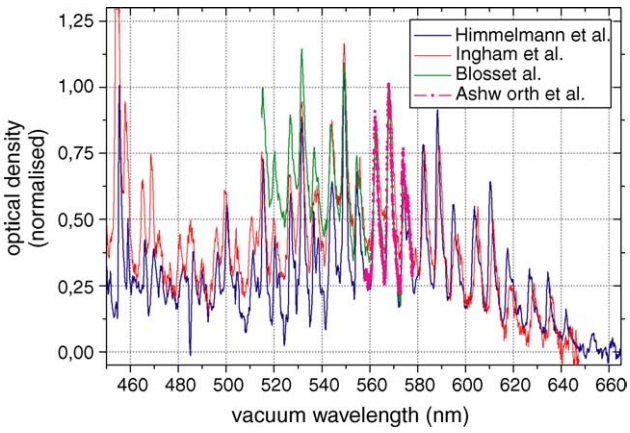

Fig. 2. The available spectra of OIO are compared. Spectra were scaled to each other in the region between 520 and 560 nm. Relative to each other the broad range spectra by Himmelmann et al. [12] and Ingham et al. [8] and the narrow range spectrum by Bloss et al. [9] show significant disagreement in background absorption. The triplet by Ashworth et al. [16] covers the scaling region, where some agreement is found between the four spectra.

(IO, OIO) at moderate resolution of the order of 0.3–1.1 nm FWHM. And secondly high resolution measurements focussing on selected bands or transitions one at a time using cavity ring down spectroscopy (CRDS), laser induced fluorescence (LIF) or submillimeter spectroscopy. The studies by [10,11] are exceptional in that they report spectra covering a larger number of ro-vibrational bands *simultaneously*, which at the same time were recorded at high resolution enabling rotational analysis. They used a 21 ft grating spectrometer and photographic plates.

As iodine oxides are only observed as transient absorbers with short lifetimes, the observational data usually consists of overlapping absorptions caused by the iodine oxides themselves, the precursors as well as all other products formed in the course of reactions. Towards longer reaction times the aerosol formation might become an issue. Also technical drift effects of light source, chemical system or others have to be considered. Due to these experimental limitations and the methods used for analysis, the spectra obtained within the first group of publications all contain more or less strong unknown background absorptions. Even though the main vibrational bands within the electronic transition might be readily visible in the reported spectra, the amount of any possibly present continuous absorption within the molecules spectrum remains in large parts unclear. The general shape of the spectrum is only insufficiently determined. This is illustrated by the comparison of available spectra for IO (Fig. 1) and OIO (Fig. 2). In the same way any continuous absorptions possibly originating from other molecules (esp. higher iodine oxides) remain hidden in the unknown background absorptions. Due to the limited spectral coverage of the high resolution studies these also fail to determine the general shape of the electronic spectra as well as in the detection of continuous absorbers.

As a result of the incomplete knowledge of the *continuous part* within an absorber's spectrum the necessary scaling of such relative spectra to an elsewhere determined *single wavelength* absolute absorption cross-section directly leads to an uncertainty in *differential absolute absorption cross-section*. This limits the accuracy of any spectroscopic determination of molecule concentration, be it in the lab or in atmospheric remote sensing as zenith sky measurements or differential optical absorption spectroscopy DOAS [19,20 and references therein].

As an attempt to minimise such problems – as well as related problems in determinations of rate coefficients and absolute absorption cross-sections – we developed a method which enables separation of absorptions originating from different molecules as well as from instrumental effects (see [21,22]). In the accompanying paper by Gómez Martín et al. [23] this method was applied to time resolved absorption spectroscopy measurements. The objective was to determine a consistent set of *single wavelength* absolute absorption cross-sections of iodine oxides detected in $I_2 + O_3$ flash photolysis experiments. The data was recorded with a grating spectrometer and a CCD camera operated in time resolved mode. For each recorded data set the separation technique produced curves of temporal behaviour of optical density for all absorbers detected. As shown in [21] these curves are to a high degree (±3%) free of interference from other absorptions and technical artefacts. They in turn provide the necessary input for the determination of single wavelength absorption cross-sections by the method of iodine conservation.

Using the curves of optical density determined there and also similar techniques, the objective of this work is to obtain likewise pure *spectra* of all absorbers detectable in $I_2 + O_3$ photolysis experiments. This improves our knowledge of the continuous absorptions within the spectra of IO and OIO and enables determination of spectra of other iodine oxides possibly occurring. Uncertainties in differential absorption cross-section of IO and OIO relevant in spectroscopic determination of molecule concentration are reduced correspondingly.

In the first half of this paper the new spectra will be presented and compared to the available literature data. A recommendation will be given. The spectrum of IO had been thoroughly analysed and will be discussed in the second half of the paper. From the analysis of the IO continuum absorption two bound-free absorp-

tion transitions within the IO molecule can be inferred. From the separated spectra of IO in differently excited vibrational states experimental Franck–Condon factors for the IO molecule are obtained.

2. Experimental set-up and origin of data

The experiment is described in detail in Section 2 of the accompanying paper [23]. There, arrays of optical density as a function of wavelength and time were obtained from the recorded intensities according to a variant of the Beer–Lambert law (for definitions see Eqs. (I-i), (I-iv), (I-vii) and (I-viii) of that paper[1]) which nicely illustrates the linear superposition of absorption of absorbers $M = 1$ to n:

$$a(\lambda, t) = \ln\left(\frac{I_0(\lambda, t)}{I(\lambda, t)}\right) = L\sum_{M=1}^{n} c_M(t)\sigma_M(\lambda) \quad \text{(i)}$$

Separation of overlapping absorptions produced curves of temporal behaviour of optical density $a_M(\lambda_M, t)$ for each absorber M detected in the experimental data and given with respect to a selected wavelength λ_M:

$$a(\lambda, t) = \sum_{M=1}^{n} a_M(\lambda_M, t)\hat{\sigma}_M(\lambda) \quad \text{(ii)}$$

$\hat{\sigma}_M(\lambda)$ denominates the (dimensionless) absorber's cross-section spectrum normalised to $\sigma_M(\lambda_M)$. The experimental data $a(\lambda, t)$ and the separated curves of temporal behaviour of optical density $a_M(\lambda_M, t)$ for all absorbers M as described and obtained in [23] provide the basis for the extraction of spectra covered in the present work. All spectra were obtained at room temperature.

3. Extraction of spectra

3.1. Theory and method

To enable usage of multiple multivariate linear regression, the observational data $a(\lambda, t)$ can be interpreted as a matrix denominated as the observational matrix $\boldsymbol{Y}$ and the curves of temporal behaviour $a_M(\lambda_M, t)$ as column vectors $\boldsymbol{a}_M$. By arranging these as columns of the so-called mixing matrix $\boldsymbol{A} = [\boldsymbol{a}_1, \boldsymbol{a}_2, \ldots, \boldsymbol{a}_n]$, Eq. (ii) can be stated in the form:

$$\boldsymbol{Y} = \sum_{M=1}^{n} \boldsymbol{a}_M \cdot \boldsymbol{s}_M^{\mathrm{T}} + \boldsymbol{E} \equiv \boldsymbol{A} \cdot \boldsymbol{S} + \boldsymbol{E} \quad \text{(iii)}$$

where $\boldsymbol{s}_M$ is a vector containing the normalised spectrum $\hat{\sigma}_M(\lambda)$ and $\boldsymbol{E}$ is the matrix of the prediction error. Because $a_M(\lambda_M, t)$ is the optical density at λ_M, the spectrum $\hat{\sigma}_M$ is normalised to unity at that wavelength (indicated by hat symbol "$\hat{\ }$"). For $\boldsymbol{s}_M$ and $\boldsymbol{S}$ the superscript is dropped, as there is no risk of confusion. Optical density is normalised to unit pathlength and the variable L is therefore omitted. Extraction of spectra is achieved by estimating $\boldsymbol{S}$ (containing the spectra as rows) given the observational data $\boldsymbol{Y}$ and the mixing matrix $\boldsymbol{A}$. The general solution to this problem (without weighting) is

$$\boldsymbol{S} = (\boldsymbol{A}^{\mathrm{T}} \cdot \boldsymbol{A})^{-1} \cdot \boldsymbol{A}^{\mathrm{T}} \cdot \boldsymbol{Y} \quad \text{(iv)}$$

Whether this solution exists or not and how accurate it is, depends on whether the columns of $\boldsymbol{A}$ are altogether linearly independent or not. The clearer the linear independence, the smaller the uncertainty in the estimated spectra $\boldsymbol{S}$. If two or more absorbers contained in the observational data $\boldsymbol{Y}$ have similar temporal behaviour or in linear combination make up a curve similar to that of another one, the solution according to (iv) is limited if not impossible. Such dependences between columns of $\boldsymbol{A}$ are referred to as multicollinearities.

If multicollinearities exist in $\boldsymbol{A}$, this will cause at least one of the eigenvalues of the normal matrix $\boldsymbol{N} \equiv \boldsymbol{A}^{\mathrm{T}} \cdot \boldsymbol{A}$ to tend to zero letting the condition number (ratio of largest to smallest eigenvalue) tend to infinity. The inverse of $\boldsymbol{N}$ will be poorly or not at all determined. The problem is said to be "ill-conditioned". According to Dahlquist et al. [24] the errors in $\boldsymbol{S}$, which originate from errors in the observational data $\boldsymbol{Y}$ as well as in the data constituting the mixing matrix $\boldsymbol{A}$ (here: the curves of temporal behaviour of absorbers) are amplified by the condition number of $\boldsymbol{N}$. In case that an inverse of $\boldsymbol{N}$ can be determined, the square root of its diagonal elements multiplied by the error of the entries into $\boldsymbol{A}$ directly equals the standard error of the estimated unknowns. Note that this simplified statement is only true, if the errors in $\boldsymbol{A}$ are constant, or in the lack of a better estimate, are assumed to be constant.

Multicollinearities can to a certain degree be avoided by appropriate selection of a subset of data, i.e. of an appropriate spectral window. This should be selected such that absorptions of one or more absorbers contributing to the multicollinearities are not contained in it, i.e. the absorption spectra of these absorbers should be zero within its range. This allows to remove the corresponding columns $\boldsymbol{a}_M$ from $\boldsymbol{A}$. The number of unknown spectra within the window is likewise reduced. As a clear drawback this directly reduces the range of the obtained spectra. For the excluded sections another extraction needs to be performed, possibly compromising on quality of the extraction. Spectra of full coverage are obtained by joining the partial spectra from the individual spectral windows accordingly.

3.2. Reliability of an obtained solution

To estimate the reliability of an obtained solution, in first place the aforementioned standard error obtained for $\boldsymbol{s}_M$ is a good measure for assessing the extent of possible multicollinearities. With respect to the shape of the obtained solutions, the non-negativity condition for absorption spectra needs to be checked. As long as emission can be excluded, all absorption spectra must be purely positive. The situation is slightly different, if data is centred to pre-flash conditions, i.e. optical density observed before the flash is averaged in time and then subtracted from all optical density data recorded in time. The resulting difference *before* the flash is equal to zero except for noise and *after* the

[1] Prefix "I-" indicates references to equations or reactions in the accompanying paper [23].

flash describes changes in optical density – i.e. concentration of precursors as well as products formed by reaction – relative to pre-flash concentrations. This also eliminates long term lamp drift very effectively. Due to this procedure also negative absorptions can occur as a result of pre-cursor consumption, but they must be *purely* negative. Spectra with mixed positive and negative sections are impossible. If such mixed solutions occur in any of the estimated spectra, this indicates systematic problems in the whole separation as such. Likewise systematic structures in the remaining residuals contained in $\boldsymbol{E}$ indicate similar problems while residuals distributed normally are a necessary indicator of a good separation. The quality of separation is further verified by comparing spectra obtained from different data sets recorded under significantly different conditions.

3.3. Uncertainty estimate for obtained spectra

The uncertainty stated for the extracted spectra is based on the estimated error of observations, i.e. optical densities. It was determined from the absorption measurements obtained during the pre-flash interval after subtraction of the pre-flash average in time, see above. In an artificial way this data is free of absorptions except for noise. The standard deviation determined in this data array was used as an estimate of the observational error, which was needed as input for the *separation of time curves* and the estimation of their error [23]. In the *extraction of spectra* (this work) by multiple multivariate linear regression two variants of errors were calculated. Firstly the error estimate of $\boldsymbol{a}_M$ (the curves of temporal behaviour of optical density as obtained in [23]) was used to vary the entries into the mixing matrix $\boldsymbol{A}$ into both directions by addition and subtraction of this error. Then the regression was solved for each case. The effect on the solutions $\boldsymbol{s}_M$ (spectra) obtained for the different variations was used as an estimate for the error propagated into the estimated spectra. Secondly an error estimate for the spectra was determined without any a priori estimate of the error assuming constant unit weight for all coefficients of the mixing matrix. This error estimate is therefore a purely statistical error estimate based on the condition of the normal matrix. Whichever was larger was used as the conservative uncertainty estimate for the resulting estimated spectra. A relative uncertainty was calculated as the ratio between the estimated uncertainty and the determined spectra. Wherever the spectra are of zero or near zero absorption, the relative uncertainty increases correspondingly. For such cases the *absolute* uncertainty will be given.

3.4. Extracted spectra

In the visible and NIR 53 data sets of time resolved flash photolysis experiments recorded under various conditions (Table 2 in [23]) were analysed covering two different spectral ranges of 280–600 and 340–660 nm. Focussing on unknown UV-absorbers two further data sets were examined, which cover 210–410 nm. Spectra obtained from different data sets were finally averaged within appropriate sections. In the averaging the estimated error was used as weight and the error of the result was determined accordingly. The method used for the determination of absolute absorption cross-sections in [23] required broad spectral coverage so that as a trade off resolution had to be low at 1.3 nm FWHM.

Absorptions from ground state IO($\nu' \leftarrow 0$), vibrationally excited IO($\nu' \leftarrow 1$) (denoted as "IO*") and IO($\nu' \leftarrow \nu''$), $\nu'' > 1$ ("IO**"), OIO, and three further absorbers with unstructured, continuous spectra labelled "X", "Y", and "Z" were found to be relevant in our experiments (nomenclature as defined in [23]). Vibrationally excited IO dominantly occurred in low pressure data. Also "X" and "Y" displayed clear dependence on conditions. Therefore in general the mixing matrix was defined as $\boldsymbol{A} = [\boldsymbol{a}_{\mathrm{IO}}, \boldsymbol{a}_{\mathrm{IO}^*}, \boldsymbol{a}_{\mathrm{IO}^{**}}, \boldsymbol{a}_{\mathrm{OIO}}, \boldsymbol{a}_{\mathrm{X}}, \boldsymbol{a}_{\mathrm{Y}}, \boldsymbol{a}_{\mathrm{Z}}]$. But depending on the individual experiment and the selected spectral interval the columns in $\boldsymbol{A}$ had to be chosen appropriately.

3.4.1. Ground state IO($\nu' \leftarrow 0$)

3.4.1.1. Other overlapping absorptions and extraction procedure. From the studies of Durie et al [11] the position of the IO($0 \leftarrow 0$) transition is known to be at 465.5 nm marking the end of the ground state IO absorption spectrum towards the red side. The observations by Himmelmann et al. [12] showed that in that region the absorptions of OIO already overlap with those of IO. Furthermore significant absorptions arising from vibrationally excited IO($\nu' \leftarrow \nu''$) with $0 < \nu'' < 7$ reach far into the OIO region [21,23]. The temporal behaviours of concentration of differently vibrationally excited species of IO depended on the experiment's conditions and the largest difference occurs between $\nu'' = 0$ and $\nu'' > 0$. IO in ground state and in vibrationally excited state therefore have to be treated as two individual species rather than a composite, averaged IO spectrum. As different behaviour in time is the key to separation, it was promising to try a separation of ground state and vibrationally excited IO spectra even though the similarity of the temporal profiles – both displaying similar rise and decay times – is a limiting factor with respect to collinearity. The temporal behaviour of overlapping OIO always showed a slower formation than the IO species. Contribution of I_2 present in the same region is unproblematic as the temporal behaviour of I_2 is totally different from that of the transient absorptions of the iodine oxides. If collinearities between ground state and vibrationally excited IO caused problems in the extraction of a *ground state* IO spectrum, a limitation of the spectral window to 467 nm on the red side always was a suitable measure, just including the last ground state band IO($0 \leftarrow 0$) and excluding the majority of IO($\nu' \leftarrow \nu''$), $\nu'' > 0$. The same collinearities could also be reduced and even avoided by analysing only data sets obtained at high pressures, in which excited IO was significantly reduced by collisional quenching.

Towards the UV the IO absorption ends in the vicinity of 320–330 nm. Varying the UV side of the extraction interval helped to verify this. Starting from 460 nm towards the UV the smooth absorption of "Z" becomes more and more important, which slowly rises in time indicating that it is caused by a product of the IO and OIO consumption mechanism. Its temporal behaviour could be obtained directly from the range around 320 nm, where no other absorptions were detected. In some cases

its contribution did not become important above 420 nm due to the flat tail of its spectrum.

3.4.1.2. Anomalous behaviour of IO(2 ← 0). In a large number of measurements apparent temporal behaviour of the IO(2 ← 0) absorption band differed significantly from that of all other bands of the ($\nu' \leftarrow 0$) progression in that the peak of IO(2 ← 0) at maximum IO concentration appeared weaker than the remaining bands. It appeared smallest in low pressure experiments and recovers systematically when proceeding to higher pressure experiments. Strong UV-photolysis (no filters between vessel and flash lamps) weakens the apparent height of the IO(2 ← 0) band further. This weakening is strongest near the time of maximum concentration. Later on the deviation dies off.

The observed difference in temporal behaviour complicated extraction of spectra. It could only be achieved by subdividing the extraction window such that in one version the (2 ← 0) band was included and in another not. Fig. 3 shows the uncorrected extraction for IO($\nu' \leftarrow 0$) including $\nu'' = 2$ (top, solid line, all extraction windows joint) and the separately extracted IO(2 ← 0) band with traces of IO(3 ← 0) (middle). In the bottom graph the relative error for the extracted spectrum of IO($\nu' \leftarrow 0$) is plotted.

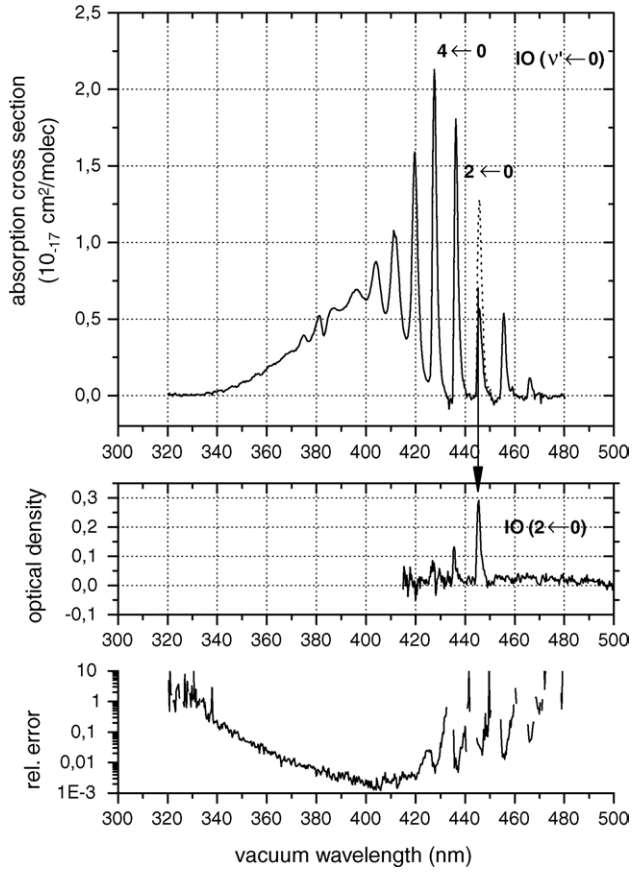

Fig. 3. The extracted spectrum of ground state IO is shown (top panel) including the apparently lower IO(2 ← 0) band before (solid line) and after correction (dotted line). In the middle panel the extraction for the anomalously behaving bands IO(2 ← 0), IO(3 ← 0) is plotted. The relative uncertainty of the IO($\nu' \leftarrow 0$) spectrum is shown in the bottom diagram. Between bands and at the ends of the spectrum the *absolute* uncertainty is of the order of (1–2) × 10^{-3} with maximum absorption at IO(4 ← 0) of 0.5, both in units of optical density.

Even without knowing the origin of the observed deviation, it is possible to estimate the correct peak height of IO(2 ← 0) relative to that of IO(4 ← 0). Calculation of the ratio of temporal behaviour of both bands verifies that the deviation dies off at times beyond the half-life of IO so that in that time range the correct ratio between peaks is obtained. The corrected IO(2 ← 0) band is plotted in Fig. 3 (top, dotted line at (2 ← 0)). After correction IO(2 ← 0) fits well within a common envelope of the ($\nu' \leftarrow 0$) progression.

3.4.1.3. Uncertainty and reproducibility. For the spectrum of IO($\nu' \leftarrow 0$) the obtained *relative* error from above 360 nm was generally less than 2.5%. Within the band maxima is of the order of 1–2%. Between the bands, where the absorption goes to zero, the *absolute* error is of the order of (0.5–2) × 10^{-3} in units of optical density compared to 0.45 in the band maximum. It increases systematically within the range, where the most serious collinearities between the different species occur.

The reproducibility of the successful extractions of spectra obtained for more than 40 data sets was very high. Systematic contradictions occurred only whenever the spectral window for the extraction was inadequately chosen and included absorptions causing collinearity or being unaccounted for by the chosen curves of temporal behaviour. Another source for systematic deviations between extractions was the build up of deposit during the flash photolysis experiments. The deposit increased within the accumulation from flash to flash and also was changed by the flash itself. In such cases the spectral window had to be reduced on the UV side. Nevertheless in some extractions of the IO spectrum systematic deviations occurred relative to the large number of consistent spectra obtained from other data sets. In spite of the deviations the UV tail of these spectra returned properly to zero. The deviations were always located at the UV side of the IO continuum. Still all extractions were introduced into the averaging for the final IO spectrum, because the origin of the deviations could not unequivocally be attributed to a gross error. But as the estimated errors of the problematic extractions were generally poorer due to the lower quality of the extraction, they entered with a lower weight into the final averaging.

3.4.1.4. Wavelength calibration. The calibration of wavelength axis had been obtained by calibration to the known positions of mercury and cadmium lines from a line source. Used were only lines well separated from others under the low resolving spectroscopic conditions of the experiment (1.3 nm FWHM). All wavelengths are converted to *vacuum wavelengths*. The accuracy of the calibration was always better than 1 pixel, which is 0.32 nm/0.26 μm geometric pixel size with the 150 grooves/mm grating. This was also verified by the wavelength offsets found between spectra of IO obtained from different data sets. In most cases the scatter in wavelength was of the order of 0.1 nm and less and of 0.2 nm as worst case. The calibration in the ground state bands was verified by comparison to the Cavity Ring-down (CRD) spectra reported by Newman et al. [14]. Their (vacuum) CRD spectra were convoluted and integrated (binned) to the res-

olution and detector geometry of our measurements and used as a calibration standard within the interval covered by them. Deviations between our spectrum and the convoluted bands from [14] ranged from −0.08 to +0.07 nm for the isolated (0 ← 0) to (4 ← 0) bands. The (5 ← 0) band was ignored, as it is likely to be distorted by the neighbouring IO continuum absorption. The instrument's function used in the convolution was only approximated by a gaussian of 1.2 nm FWHM (*not* gaussian half width). This was estimated from the FWHM of the apparent line shape obtained from a line source measurement. Therefore the differences between the convoluted CRD spectra and our spectrum were not used for re-calibration. Nevertheless the differences lying clearly below 0.1 nm justify a conservative (but nevertheless sub-pixel) estimate of wavelength uncertainty of 0.2 nm.

The apparent positions of band maxima will differ more or less strongly depending on the difference in resolution and binning, e.g. IO(4 ← 0) in the CRDS study by [14] at 427.2 nm (vac.) versus 427.5 nm (vac.) from this work at 1.3 nm FWHM. This is explained by the fact that lower resolution and binning cause the peak of an asymmetric band to be shifted away from the steepest ascend. This can be verified by corresponding simulations and was also verified by the convolution and binning of the data of [14].

3.4.2. Vibrationally excited IO($\nu' \leftarrow \nu''$) with $\nu'' > 0$

3.4.2.1. Other overlapping absorptions and separation procedure. In the spectral window from 467 to 600 nm the contributions of vibrationally excited IO($\nu' \leftarrow \nu''$), $\nu'' > 0$, of OIO and of I_2 could be separated from each other with low errors wherever the individual spectrum has significant absorption. Collinearities with the ground state of IO were avoided by excluding the IO(0 ← 0) at 465.5 nm from the spectral window. By limiting the spectral window to 480–600 nm this could be improved even more, because then IO($\nu' \leftarrow 1$), the temporal behaviour of which differed from that of IO($\nu' \leftarrow \nu''$), $\nu'' > 1$, was also excluded. Especially the low pressure data sets containing the largest concentrations of excited IO yielded clear spectra. For the bands falling between those of the ground state of IO, i.e. below 467 nm, the separation proved to be more difficult, as there the similarity of temporal behaviour of the ground state of IO in general, that of IO(2 ← 0) and that of excited IO produces multicollinearities and imperfect extraction of individual spectra. On the other hand the temporal behaviours were sufficiently different to inhibit a reduction of free parameters. In this interval the noise in the extracted spectra is larger and negative traces of the ground state of IO remain. Below 440 nm again the absorption of absorber "Z" needs to be taken into account. Also in a number of data sets the absorption caused by "X" found between 320 and 420 nm (see [23]) proved to be significant. Due to its temporal behaviour being similar – but not completely the same – to that of IO($\nu' \leftarrow \nu''$), $\nu'' > 1$, its spectrum was in many fits extracted together with the bands of excited IO as a single spectrum with acceptable residuals, see Fig. 4. Its spectrum displays a smooth continuum located in the region of the ground state IO continuum.

The temporal resolution of our set-up is defined on one hand by the shifting time per row of the CCD chip and on the other hand by the characteristic function in time (defined by the masking of the chip and the vertical slit width of the mask). The characteristic function has a half width of 5–7 pixels in different regions of the chip. The variations are caused by mechanical imperfections of the laboratory-made masking of the chip. The difference between temporal behaviour of excited IO and that of the found absorption "X" is visible only in a time interval of 10–12 pixels in time – roughly twice the width of the instrument's characteristic function in time – and very close to the flash. The large remainder of both curves is nearly identical. Therefore it is possible that the observed continuum belongs to excited IO. But on the other hand it cannot be excluded that it originates from a further not yet identified species. This can only be decided after further analysis of spectra, see below. The full spectrum extracted for vibrationally excited IO obtained by joining the three different sections is shown in Fig. 4. In the bottom graph the obtained relative uncertainty is plotted.

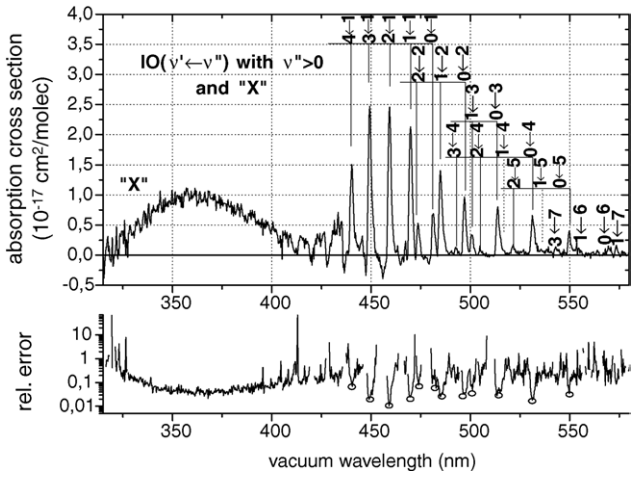

Fig. 4. For vibrationally excited IO a spectrum was obtained by joining three sections from three extraction intervals (top). The continuum absorption (labelled "X") is of unclear origin, to be discussed below. Band assignments are according to [11]. The relative uncertainty of the extracted spectrum is shown in the bottom diagram. Open circles indicate the relative uncertainty at band maxima. Between bands and at the ends of the spectrum the *absolute* uncertainty is of the order of (2–5) × 10^{-4} with maximum absorption at IO(3 ← 1) of 0.025, both in units of optical density.

3.4.2.2. Uncertainty and reproducibility. The reproducibility of the spectrum was highest in the range from 480 to 600 nm. The shape of the bands and zero absorption in the troughs was always reproduced. Depending on the mixture changes in relative height between groups of bands from different ν'' occurred. When the window was extended down to 467 nm and below, the different behaviour of IO($\nu' \leftarrow 1$) and IO(0 ← 0) reduced the reproducibility in that traces of the ground state of IO appeared in the spectrum or a continuous background disturbed the spectrum. In the continuum ("X") in spite of the low signal to noise the reproducibility was good. Based on the error estimate the uncertainty of the spectrum is approximately 2–3% in the peaks. In the continuum range it is of the order of 5–10%. Between the bands the *absolute* error is of the order of (2–5) × 10^{-4} in units of optical density.

3.4.2.3. Wavelength calibration. The wavelength calibration for vibrationally excited IO is the same as described for the ground state of IO.

3.4.2.4. Assignment of transitions. In 1958 Durie and Ramsay [10] recorded bands of IO in *absorption*, where only ground state IO($\nu' \leftarrow 0$) and the IO($2 \leftarrow 1$) band were visible. In 1960 Durie et al. [11] carefully examined the *emission* spectrum of IO using a 21 ft grating spectrometer in second or higher order and observed a large number of transitions from vibrationally excited IO. They performed a thorough rotational and vibrational analysis, which enabled determination of the band *origins* of both ground state and vibrationally excited IO. From the band origins they determined vibrational constants for IO, with residuals generally better than 0.005 nm. Only overlapped bands were reproduced with larger residuals of 0.02–0.03 nm.

In our low resolution measurements for the first time a large number of vibrationally excited bands are observed in *absorption*. In our extracted absorption spectrum 22 bands of excited IO are present out of 34 observed by Durie et al. [11] in emission, see Fig. 4 with the assignments according to [11]. As our measurements were aimed at broad and simultaneous spectral coverage, high resolution was not the point of our work. Given the limited resolution of 1.3 nm FWHM and 0.35 nm/pixel of our measurements, our band *maxima* are in reasonable agreement with their accurate band *origins*.

Examination of band height of individual progressions shows that in the IO($\nu' \leftarrow 1$) similar as in the $\nu'' = 0$ series again the transition leading to the $A^2\Pi_{3/2}$, $\nu' = 2$ appears to be weakened in comparison to the neighbouring bands of the same series (see Fig. 4). This agrees to the observed anomaly being linked to the $A^2\Pi_{3/2}$, $\nu' = 2$ state. A more quantitative statement about this was not possible, because firstly collinearities impeded the separation of temporal behaviour of IO($2 \leftarrow 1$) from the remaining IO($\nu' \leftarrow 1$) bands. Secondly the time scale of formation of these excited species was at and below the temporal resolution of our set-up. The other interesting feature is the strong and regular presence of the IO($0 \leftarrow \nu''$) transitions. Starting with the barely visible ($0 \leftarrow 6$) band, the bands increase steadily until the ($0 \leftarrow 2$) band, before decreasing in the ($0 \leftarrow 1$) band again.

3.4.3. OIO(0, ν_2', $\nu_3' \leftarrow$ 0, 0, 0)

Between 480 and 600 nm the spectrum of OIO could be extracted without problems, as no collinearities between OIO, IO($\nu' \leftarrow \nu''$), $\nu'' > 1$ and I_2 occurred. Below 480 nm the problems of extraction were those described above for vibrationally excited IO. The quality of the extracted spectrum is correspondingly lower than between 480 and 600 nm. Nevertheless the blue end of the OIO spectrum is well defined, see Fig. 5. Some negative contributions caused by imperfect separation from IO($2 \leftarrow 1$) and IO($3 \leftarrow 1$) remain, but the pattern of band triplets caused by the OIO angle bend of vibrational levels ν_3' ranging from 0 to 2 up to OIO(0, 10, $1 \leftarrow 0, 0, 0$) is clearly present (notation: ν_1, ν_2, ν_3: asymmetric stretch, symmetric stretch, angle bend). To the red the interval from 600 to 660 nm was covered by a limited number of experiments of at the same time limited signal to noise due to technical imperfections. Therefore

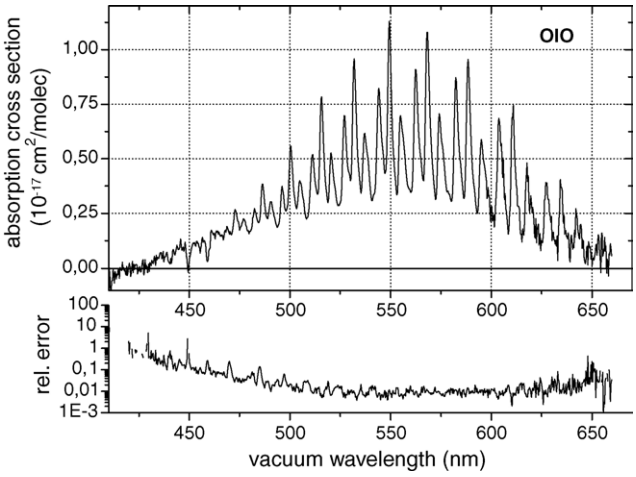

Fig. 5. The spectrum of OIO was extracted from three different sections and then joined to form a contiguous spectrum. On both sides it shows a clear and smooth return to zero. Band triplets and the envelope of the spectrum show a systematic form. The bottom diagram shows the relative uncertainty of the spectrum. At the ends of the spectrum the *absolute* uncertainty is of the order of $(0.3–1) \times 10^{-3}$ with maximum absorption at OIO(0, 5, 1) of 0.08, both in units of optical density.

the data quality in that range in spite of the absence of collinearity problems is lower than in the 460–600 nm range. Still the red tail of the spectrum is quite well determined.

3.4.3.1. Uncertainty and reproducibility. As for vibrationally excited IO the reproducibility of the spectrum was highest in the range from 480 to 600 nm. From 470 to 600 nm the relative error is clearly below 5%, in many parts even at and around 1%. Larger errors occur at wavelengths, where bands of vibrationally excited IO are located. Above 600 nm the error estimate varies strongly between a few percent and up to 15% due to the lower data quality. Below 470 nm the *absolute* error was always of the order of a few percent of the maximum absorption in the (0, 5, $1 \leftarrow 0$, 0, 0) band. The shape of the bands and especially the depth of the absorption minima between bands were always reproduced, strongly supporting the assumed quality of separation of no more than ±3% foreign contributions from other absorbers [21].

3.4.3.2. Wavelength calibration. As the spectra were all obtained from the same data the wavelength calibration for OIO is the same one as described above.

3.4.4. Further UV–vis absorbers "X", "Y", and "Z"

The extraction of absorber "X" was described in the context of vibrationally excited IO. Its origin remains to be clarified, see below. Absorbers "Y" and "Z" were already obtained in the separation of curves of temporal behaviour as described in the accompanying paper [23]. Fig. 6 compares the spectra obtained for "X", "Y" and "Z" obtained from the majority of data sets, which were centred on the visible range ($\lambda > 300$ nm). They are already scaled to absolute absorption cross-sections. In [23] these were determined per iodine atom contained in the molecule. The spectra presented in this section are scaled assuming a stoichiometry of I_2O_2 for "Y" (see [23]). Also for "Z"

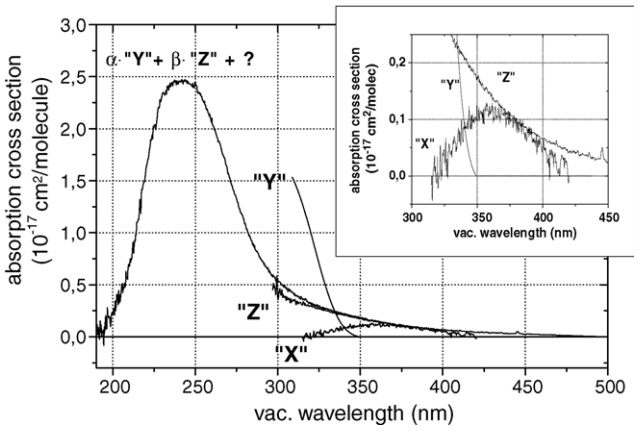

Fig. 6. Three further absorptions were found in the UV and visible, labelled "X", "Y", and "Z". Absorption "Y" was smoothed (scatter of original data: $\pm 1.2 \times 10^{-18}$ cm^2/molecules). Spectra are scaled to absolute cross-sections according to [23] and assuming two iodine atoms per molecule for "Y" and "Z" and one iodine atom per molecule for "X". Further to the UV an absorption was extracted from measurements, which is likely to be a superposition of "Y" and "Z" and possibly a third absorber. This is scaled at the red end to "Z".

a molecule that contains only two iodine atoms was assumed, on the grounds that it appears on a similar time scale as "Y", see temporal behaviours in [23]. For "X" only one iodine atom was assumed for reasons to be discussed below. Even with having this factor of two in mind the absorption cross-section of "X" clearly is the smallest of the three spectra found in this analysis.

From the two further data sets covering 210–410 nm a composite spectrum of an UV absorption was separated from the underlying ozone absorption using the DOAS technique in the Hartley band and multiple multivariate linear regression. There is evidence that the obtained spectrum (Fig. 6, $\lambda < 300$ nm) is a superposition of two absorbers, possibly "Y" and "Z" not excluding the presence of possibly a third one.

All spectra obtained in this work are available as supplementary data alongside the electronic version of this article as published in Elsevier Web Products.

3.5. Discussion

3.5.1. Ground state and vibrationally excited IO

The spectrum obtained for ground state IO($\nu' \leftarrow 0$) is free of negative absorptions proving that no systematic problems in the extraction exist. Only in the absorption minima some negative sections exist, clearly originating from incomplete separation from excited IO. The negative values are of the order of 2% relative to the peak absorption and therefore within the ±3% uncertainty determined for the separation. The UV-end of the spectrum is clearly determined. Superimposed to the continuum absorption, bands of small amplitude are visible belonging to the ($\nu' \leftarrow 0$) progression. They increase in amplitude near 380 nm showing a very clear band feature. From thereon to the red they first die off before becoming dominant again starting from ($6 \leftarrow 0$). The continuum absorption dies off near 430 nm. From the ($4 \leftarrow 0$) band to the ($0 \leftarrow 0$) band all absorption minima between bands return to zero within ±3%. No bands of vibrationally excited IO($\nu' \leftarrow 1$) are present due to the separation method used in our analysis.

Given the width of the spectrometer's slit function of 1.3 nm FWHM the continuum up to the ($6 \leftarrow 0$) band can be regarded as free of resolutional effects. The same holds for the main parts of the absorption minima and the red flanks of bands thereby clarifying the extent of continuous absorptions under the vibrational bands of the IO A ← X transition.

In Fig. 1 the previously published spectra of IO [5,6,9] are compared. At the maximum of the ($6 \leftarrow 0$) band near 410 nm they have been scaled to unity, which takes into account that below that wavelength the absorption by higher oxides and above that wavelength that by (depending on the mixtures) I_2, vibrationally excited IO and OIO becomes important. The ($6 \leftarrow 0$) band is sufficiently broad to avoid complications caused by different resolution.

There is disagreement among [5,6,9] with respect to the continuous background contained in the spectrum. This indicates the presence of additional continuous absorptions in their determination. The disagreement in the absorption minima (crucial for the correct differential absorption cross-section needed for DOAS) is especially remarkable. There, also peaks originating from vibrationally excited IO are found. The partitioning between ground state and vibrationally excited state bands is different among them.

Fig. 7 compares the spectra individually to the IO($\nu' \leftarrow 0$) *ground state* spectrum obtained in this work. In each case our spectrum lies in most parts clearly below the other ones indicating uncorrected background absorption in the latter. This is smallest but not negligible in the spectrum of [9], which also shows bands from vibrationally excited IO($\nu' \leftarrow 1$).

The spectrum of Laszlo et al. [5] was obtained by a scanning monochromator and photomultiplier set-up. There is no mention of any correction of background absorption except that the section below 430 nm was recorded with $O + I_2$ as source of IO and the section above with $O + CF_3I$ to avoid interference from I_2 absorption. The slit function of the monochromator was 0.3 nm (2365 grooves/mm, 200 μm slit) and the step size 0.6 nm below 400 and 0.3 nm above. Reproducibility was high excluding non-systematic effects like light source drift or instability of the chemical mixtures. Harwood et al. [6] obtained their spectrum with a 270 mm focal length spectrograph and photo diode array by comparing 50 μs averages obtained before and after the photolysis flash. The experiment was performed in the $O + CF_3I$ system. The slit function was of 0.44 nm FWHM with 0.12 nm/pixel. A correction for background absorptions was not performed. Bloss et al. [9] used an arrangement similar to ours with a 250 mm spectrograph, 300 grooves/mm grating and a CCD camera for time resolved absorption spectroscopy. Spectral coverage was 65 nm. The slit function had 1.13 nm FWHM. Experiments were performed at atmospheric pressure, so that vibrationally excited IO should be in thermal equilibrium with ground state IO. A continuous absorption spectrum (labelled "P") was determined, which arose as a product of IO and OIO consumption. A separation of this absorption into different contributions was not performed. An upper limit to the IO spectrum was obtained from spectra recorded immediately after the flash

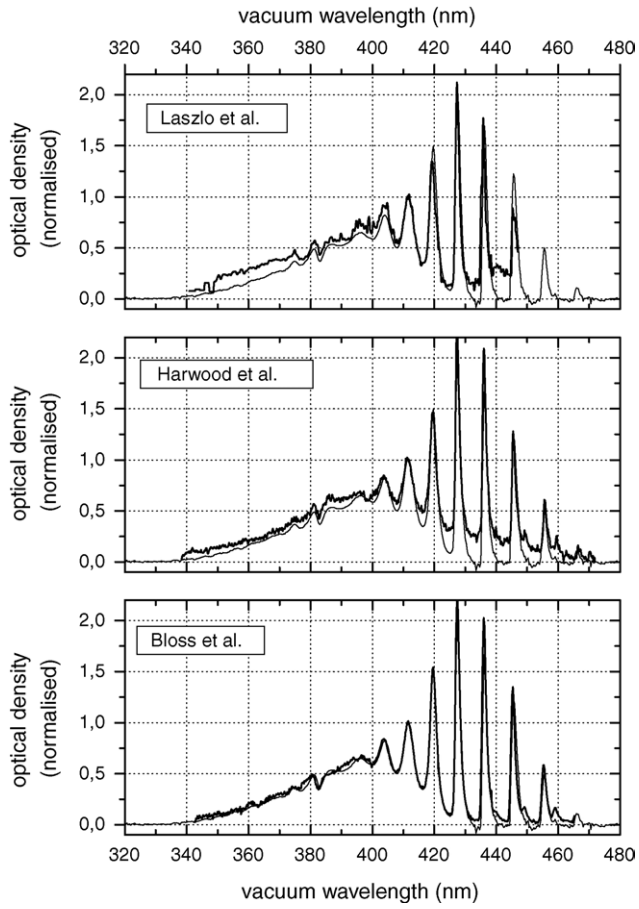

Fig. 7. The available spectra for IO (thick line) are compared to the spectrum determined in this work (thin line). While discrepancies between those by Laszlo et al. [5] and Harwood et al. [6] and our spectrum are strongest in the absorption minima, the spectrum by Bloss et al. [9] shows a much better agreement. This is in line with the fact that only in the determination of that spectrum a correction of background absorptions was performed. But still traces of uncorrected other absorptions are present.

at maximum [IO]. Product absorptions were assumed to being minimised by that. A lower limit was determined by subtraction of the scaled absorption spectrum "P" by assuming that absorption below 340 nm originated dominantly from "P" and not from IO.

As [9] is the only previous study, in which a correction for unaccounted foreign absorptions was performed, it is not surprising that the agreement between their spectrum and our IO($\nu' \leftarrow 0$) *ground state* spectrum is much better than between that of [5,6] and ours. The remaining discrepancies between the spectrum of [9] and our spectrum presumably result from (a) the approximations required by their step-wise correction, (b) the fact that the product spectrum "P" used for correction most likely is a composition of differently evolving product spectra (see above: possibly "Y" and "Z", compare also Fig. 6 in [9]), (c) the contributions of vibrationally excited IO present in their spectrum and possibly (d) the necessity of having to join the final spectrum out of different sections obtained in different experiments due to the limited spectral coverage of 65 nm.

Fig. 8 gives an example of the different data quality achieved in the continuum absorption of IO. As our spectrum is the product of analysis of 53 different data sets, the signal to noise is significantly better than in the spectra determined from less data. The vibrational structure at 380 nm is clearly resolved and the neighbouring ground state bands are clearly visible.

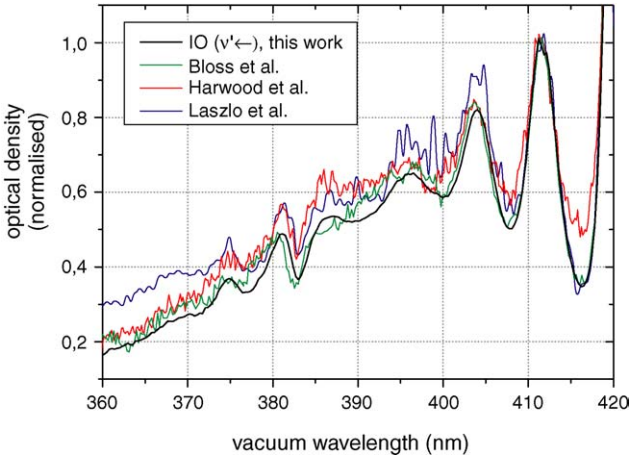

Fig. 8. A section of the IO spectrum near the vibrational feature in the absorption continuum is shown. Comparison of the IO($\nu' \leftarrow 0$) from this work to the available spectra illustrates the difference in data quality. The spectrum obtained in this work shows significantly less noise due to the extraction method, which uses practically all optical density data of measurable signal. Also the large number of available individual spectra (53 data sets), which had been averaged, reduces noise.

With respect to wavelength calibration the spectrum of Laszlo et al. [5] shows disagreement to all other spectra (including ours) with deviations of different direction between neighbouring bands. The stated high reproducibility rules out any deviation caused by limited reproducibility of wavelength during scans. Therefore these contradictions cannot be resolved. Between the spectra of [6,9] and ours the disagreement is of similar magnitude of the order of 0.1–0.5 nm in the flanks and of 0.1–0.3 nm in the band maxima increasing to the red. Both calibrated their spectra with the lines of a mercury lamp. Our spectrum was calibrated with a mercury–cadmium lamp having additional lines in the region of interest and the band positions agree within better than 0.1 nm with to the convoluted and binned bands determined by the CRDS study of Newman et al. [14], see above. This indicates that the disagreement between the spectra of [6,9] and ours could be caused by the lower number of calibration lines used in their calibration.

Summarising all aspects discussed, it is concluded that in all regions, where spectral resolution is not an issue, the spectrum obtained in this work determines the instrument independent shape of the IO ground state spectrum more accurately than the previously published spectra. In comparison to the 1.13 nm FWHM spectrum of [9] the difference to our 1.3 nm FWHM spectrum should not be a dominant effect. As by our study vibrationally excited IO is for the first time explicitly determined as an independent species, this provides the possibility of taking non-equilibrium conditions dedicatedly into account.

3.5.2. OIO

The OIO spectrum determined in this work has clearly defined ends towards the blue and the red, both dying off towards

zero. Apart from two inverted features originating from incomplete separation from vibrationally excited IO no systematic negative sections appear. This indicates that no systematic problems in the separation of spectra were present. The general pattern of band triplets is regular and also the envelope is free of irregularities.

Relative to the width of the spectrometer's slit function of 1.3 nm FWHM the most narrow bands are two to three times wider (width at half the height measured from peak to peak). The flanks are in general less steep than in the case of IO, covering roughly one FWHM. Owing to the trade-off enforced by the requirement of simultaneous coverage [22,23] the OIO spectrum is therefore close to but not yet fully instrument independent. The study of effects of resolution (MIntAS) showed that changes of the order of 14% have still to be expected in the peak absorption at OIO(0, 5, 1 ← 0, 0, 0) [22,23,25].

Fig. 2 compares the previously available spectra for OIO [8,9,12,16]. They have been scaled to unity in the top of the (0, 4, 1 ← 0, 0, 0) transition, which is the broadest maximum included in *all* spectra. Similar as for IO significant discrepancies exist in the OIO spectra with respect to uncorrected foreign background absorptions. Here the effect on differential amplitude is even more striking. This could be due to the fact that OIO absorption in most experiments is significantly smaller than that of IO (being a product of IO consumption). Uncorrected background absorptions therefore introduce correspondingly larger errors in the scaling.

The spectrum of [12] was recorded with a 500 mm grating spectrometer, a 300 grooves/mm grating and a 1024 pixel photo diode array with sequential readout. The latter causes a time shift of 16 μs from pixel to pixel and therefore roughly 16 ms between first and last pixel of a spectrum. The half-life of OIO was of the same order of magnitude. The spectrum was obtained by subtraction of appropriate spectra. A correction for background absorptions was not performed. Wavelength calibration was obtained from the lines of a mercury–cadmium line source. The spectrum by Ingham et al. [8] was recorded with a 500 mm grating spectrometer, 300 grooves/mm grating and a *gated* diode array. Spectral resolution was 0.7 nm FWHM. The spectrum was calculated based on a ratio of pre-flash to post-flash intensity. The spectrum was corrected for change in I_2 absorption due to I_2 consumption. There is no mention of correction of other background absorptions. Wavelength calibration was obtained from a mercury line source. The OIO spectrum published by Bloss et al. [9] was obtained under the conditions already described for IO. A correction of foreign background absorption *in the OIO spectrum* is not mentioned. Ashworth et al. [16] recorded the 540 to 605 nm section of the OIO spectrum by CRD spectroscopy at 0.2 cm^{-1} (≈0.006 nm). The spectrum was obtained at 100 μs delay between photolysis and probe pulse. Empty vessel CRD spectra were used to correct for instrumental effects. I_2 absorptions were corrected. Further corrections are not mentioned. A low resolution spectrum was also recorded with a 500 mm grating spectrometer, a 600 grooves/mm grating and a CCD camera. Resolution was 0.6 nm FWHM. There is no mention of correction of other background absorptions in that spectrum.

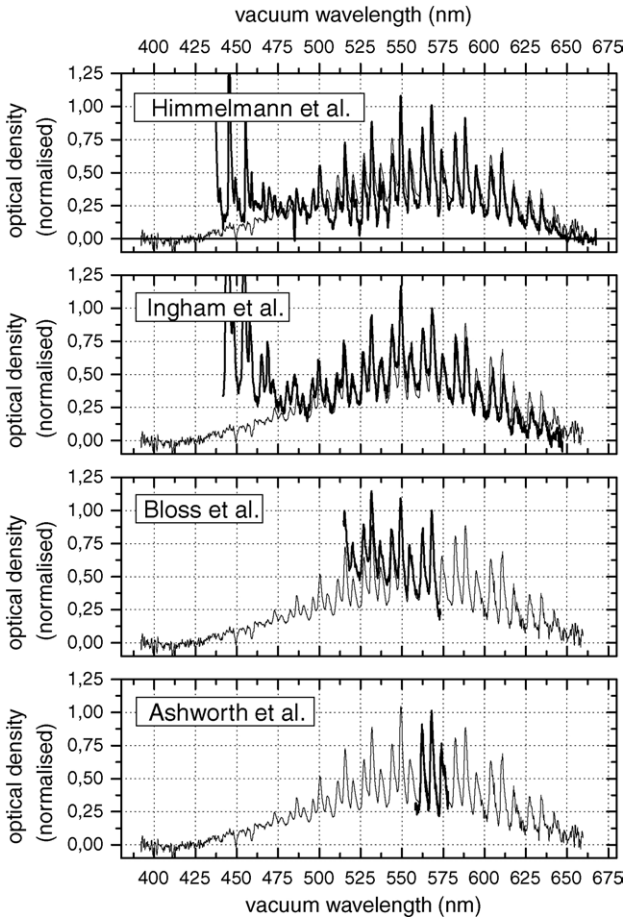

Fig. 9. The spectra available for OIO (thick line) are compared to the spectrum determined in this work (thin line). All spectra but the "single triplet"-section by Ashworth et al. [16] show considerable disagreement being caused by uncorrected background absorptions. Especially the overlap with IO bands is clearly present in the spectra of Himmelmann et al. [12] and Ingham et al. [8]. In the spectrum of Bloss et al. [9] also strong background absorption occurs even in the narrow window available.

Fig. 9 compares the available spectra individually to the one obtained in this work. Both spectra of broad coverage [8,12] are superpositions of IO and OIO. The IO bands on the blue end of the spectrum are significantly stronger than the OIO bands. The blue end of the OIO spectrum is not determined. In the IO absorption minima strong interference from a further additional continuous absorption is present in both spectra. The regular pattern of band triples is disturbed in both. In the spectrum by [12] inversed lines originating from the xenon photolysis flash and I_2 bands are present. In the spectrum by [8] absorption minima appear to be irregularly filled. Regular structures in flanks of OIO bands indicate that interference from I_2 bands is possibly present. To the red the bands are significantly reduced in strength.

The partial spectrum by [9] shows strong interference from background absorption on its blue end. Only the triplet near 560–580 nm is in reasonable agreement with our spectrum.

The partial spectrum by [16] is in good agreement with the band triplet from our work. Disagreement exists with respect to the depth of the absorption minima or rather – due to the selected

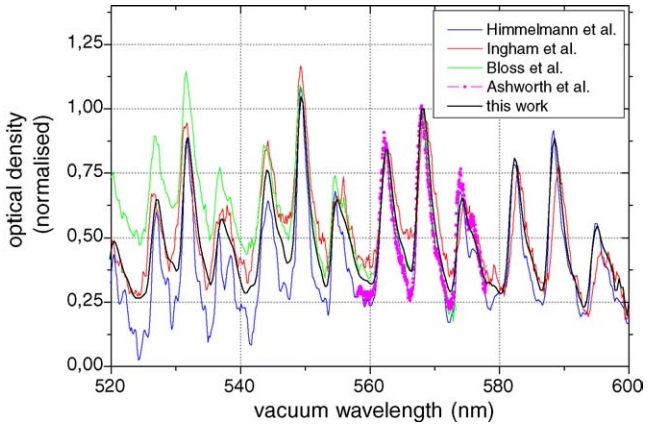

Fig. 10. A section of the OIO spectrum near the peak absorption is shown. Comparison to the available spectra illustrates the difference in data quality. The spectrum obtained in this work shows significantly less noise due to the extraction method, which uses practically all optical density data of measurable signal. Also the large number of available individual spectra (53 data sets), which had been averaged, reduces noise. Regular structures in the spectra by Himmelmann et al. [12] as well as Ingham et al. [8] indicate the presence of uncorrected absorptions caused by I_2.

scaling – with respect to the amplitude of differential structure. This is most likely a result of the significantly higher resolution of their CDRS measurement.

Fig. 10 gives an example of the different data quality achieved for the absorption spectrum of OIO. As our spectrum (with the exception of the red end) is the product of analysis of 53 different data sets, the signal to noise is significantly better than in the other spectra.

The effects associated to the lower resolution of our spectrum (14% between 1.3 and 0.35 nm FWHM at OIO(0, 5, 1 ← 0, 0, 0), see above) are less significant than the systematic effects present in [8,12]. The same holds for [9]. In addition a broader spectral range is covered. Within its narrow range of spectral coverage the CRD spectrum by [16] definitely provides an instrument independent differential spectrum. But the scaling of the *absolute differential* absorption cross-section to be derived from that spectrum remains affected by the possible presence of foreign background absorption, which cannot be completely excluded.

3.5.3. Absorbers "X", "Y", and "Z"

To our best knowledge the spectra obtained for the absorbers "Y" and "Z" are the first absorber-specific gas phase UV–vis absorption spectra reported for – what they most likely are – higher iodine oxides formed in the consumption of IO and OIO. They are free of negative sections indicating absence of systematic problems in the separation and extraction of spectra. Scaled to the absolute absorption cross-sections estimated in [22,23] they display a maximum absorption around $(2–2.5) \times 10^{-17}$ cm^2/molecules which is in reasonable agreement with the absorption cross-sections known for chlorine and bromine oxides. This also verifies that no gross error is present in the shape of the spectra, as the absolute cross-sections were determined in the flanks of the observed spectra. A comparison with the aerosol spectra reported by Harwood et al. [6] does not seem appropriate, as these were determined at time scales of 10–300 s and as a product of $I_2 + O_3$ 'dark' reaction without photolysis. Bloss et al. [9] report a product spectrum (see above: "P"), which displays a general shape very similar to "Z". The difference between their product spectra obtained in the $O + CF_3I$ system and in $O + I_2$ could be possibly caused by "Y" indicating dependence of formation of "Y" on the presence of I_2.

For the spectrum of "X" no prior reference exists. Being among the earliest absorptions observed in the $I + O_3$ photolysis, it is clear that "X" can only be caused by an early product such as e.g. $I + O_2 + M \rightarrow IOO + M$ or $I + O_3 + M \rightarrow IO_3 + M$ or possibly part of the IO absorption spectrum not originating from IO($\nu' \leftarrow 0$). This will be clarified in the following analysis of the IO absorption spectrum.

4. Analysis of the IO spectrum

4.1. Absorption continuum of ground state IO($\nu' \leftarrow 0$)

The extraction of a full range spectrum for ground state IO being practically free of other absorptions for the first time enables a clear statement about the shape and the extent of the IO continuum absorption. It starts near 330 nm and extends to the (4 ← 0) band. Important are the band structures, which are superimposed to it. Among these the localised increase of amplitude near 380 nm is of special interest.

Given the high quality of extraction it is promising to examine the origin of the observed continuum absorption. The presence of a continuum absorption indicates the existence of at least one optically active repulsive potential intersecting with the upper binding electronic $A^2\Pi_i$ potentials of the IO molecule. This is supported by the change of shape of the bands of ground state IO (Fig. 3): From (0 ← 0) to (4 ← 0) the bands display an asymmetry with pronounced steep flanks towards the blue. In the troughs absorption returns to zero. But starting with (5 ← 0), band shape steadily becomes more symmetric, width increases and height decreases and wings become more prominent resulting from overlap of broadened, Lorentz shaped rotational lines. The troughs between bands (starting between $\nu'' = 4$ and 5) no longer return to zero. So in principle the continuum could be caused by overlap of bands, which are broadened by predissociation. At and around the (10 ← 0) band the width of bands reduces significantly and height is increased again. Broadening of the vibrational bands and therefore predissociation of the corresponding upper states must be smaller than in the neighbouring states. Further towards the UV broadening increases again, with no further visible changes.

The occurrence of a region of less predissociation near (10 ← 0) indicates that at least two repulsive potentials, which intersect with the IO($A^2\Pi_{3/2}$) potential, must be of relevance to the observed continuum. One coupling dominantly to states from $\nu'' = 5$ to approximately $\nu'' = 9$ and another coupling dominantly to states $\nu'' > 10$. This is in agreement with findings by [14], who concluded from their ab initio work on ClO and from Wigner–Witmer correlation rules that a larger number of repulsive potentials is likely for IO.

4.1.1. Simulation of observed continuum: multi-parameter fit

To get an insight into the origin of the observed continuum and of the broadening of bands, it was examined, how the observed spectrum can be reproduced based on different assumptions. As this study will also involve energy considerations, the spectra from here on will be represented on a wavenumber axis instead of wavelength. Two hypotheses were considered:

Hypothesis 1. The observed continuum is caused solely by overlap of broadened vibrational bands from bound–bound transitions. Where predissociation and therefore broadening is strong, the band shape is approximated by a Lorentz profile. If necessary, *asymmetric* band profiles will be allowed. The latter is likely for the $(5 \leftarrow 0)$, $(10 \leftarrow 0)$ and possibly $v'' = 10 \pm 1$.

Hypothesis 2. The observed continuum is caused by overlap of broadened vibrational bands from bound–bound transitions and two continua originating from two bound-free transitions into two independent repulsive states. As above, asymmetric profiles will be allowed, where necessary.

Multi-parameter fitting routines were used to test the two hypotheses. With both it was possible to reproduce the shape of the observed continuum with reasonable residuals. For both cases the magnitude of individual bands relative to each other – band strength determined by the area under the band – was determined. For comparison Franck–Condon factors for the IO $A^2\Pi_{3/2} \leftarrow X^2\Pi_{3/2}$ transition were calculated in Morse approximation [26,27]. This is based on the fact that the area under each band is to a good approximation proportional to the Franck–Condon factor of the corresponding transition. The potentials were defined via ω_e and $\omega_e x_e$ with the results from Durie et al. [11]. The dissociation energy D_e was not used. Thereby it is guaranteed that the term values, the turning points and the shape of the state functions for low to mid vibrational levels agree with experimental data. Only the small effect of the $\omega_e y_e$ term is neglected.

In comparison to the calculated Franck–Condon factors neither of the two series of band strength obtained from the fits at least roughly approximated the expected systematic behaviour. It had to be concluded that the numerical fit in both cases was overparameterised. But also Hypothesis 1 could be discarded. The observed continuum *has to contain* contributions from bound-free transitions. Discarding the second fit only implies that the strength of bound-free continua was overestimated. To overcome this problem the strength of bands in the fit was constrained to the systematic behaviour of the calculated Franck–Condon factors. The corresponding fit also reproduced the observed continuum absorption with good residuals (Fig. 11). The structure near the $(10 \leftarrow 0)$ transition is somewhat poorer reproduced, which is a result of the formal limitation of the constrained fitting routine, which only allowed symmetric, Lorentz shaped bands. This is a good approximation away from the centre of bands, where the wings of Lorentz shaped rotational lines are dominant. Asymmetries in the observed bands resulting from the intensity distribution of rotational transitions near the band centre were suppressed in the model. Nevertheless the observed continuum as a whole is reproduced accurately with only small residuals.

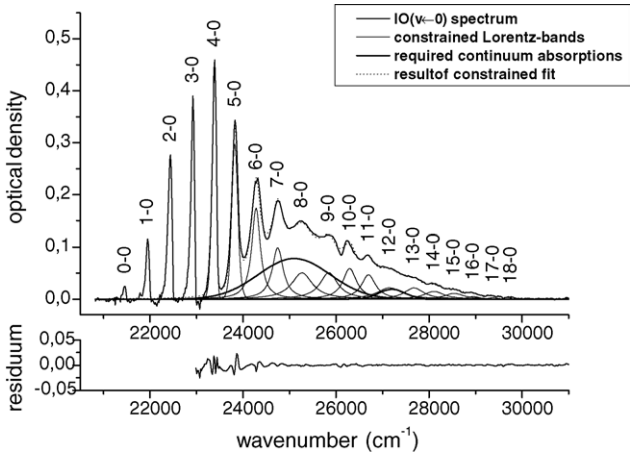

Fig. 11. The continuum of ground state IO was reproduced by assuming Lorentz shaped bands within the range of the continuum absorption. Band strength was constrained to the systematic behaviour of calculated Franck–Condon factors. In addition, two gaussian continua (green) representing two hypothetical bound-free transitions had to be included to reproduce the observed continuum. Only at bands, for which the asymmetric band shape cannot be reproduced by Lorentz bands the residuals (absolute scale) show significant structure.

The properties of the deduced bound-free transition continua are summarised in Table 1. They differ significantly in strength, i.e. area under the curve. The band strength was scaled relative to the calculated Franck–Condon factors for the bound–bound transitions. As they originate from the IO($X^2\Pi_{3/2}$) at $v'' = 0$, their origin in terms of internuclear distance is the equilibrium distance of the ground state. The value shown in Table 1 is that published in [11].

4.1.2. Deducing repulsive states from observed continua

Using the internuclear equilibrium distance at $v'' = 0$ and the centre of a spectroscopically found bound-free absorption continuum we have determined a point of the corresponding

Table 1
Two bound-free transitions are inferred from the constrained fit to the observed absorption continuum of ground state IO

	Area (cm^{-1})	Centre (cm^{-1})	Half width (cm^{-1})	Origin: $r_e(X^2\Pi_{3/2})$ (Å)
Bound-free 1	0.258 ± 0.008	25101 ± 100 (± 18)	1544 ± 37	$v'' = 0$, 1.8676
Bound-free 2	0.023 ± 0.002	27202 ± 100 (± 27)	570 ± 55	$v'' = 0$, 1.8676

A strong one with its maximum located near the $(8 \leftarrow 0)$ transition and a weaker one nearly coinciding with $(12 \leftarrow 0)$. Stated uncertainties are those, which resulted from the constrained fit indicating its stability. For the centre the error was estimated conservatively by taking the approximation of a most likely asymmetric curve by a gaussian into account, uncertainties from fit in parentheses. Band strength estimates (area) obtained from the area under the gaussians are scaled relative to the calculated Franck–Condon factors of the bound–bound transitions of the $(v' \leftarrow 0)$ progression.

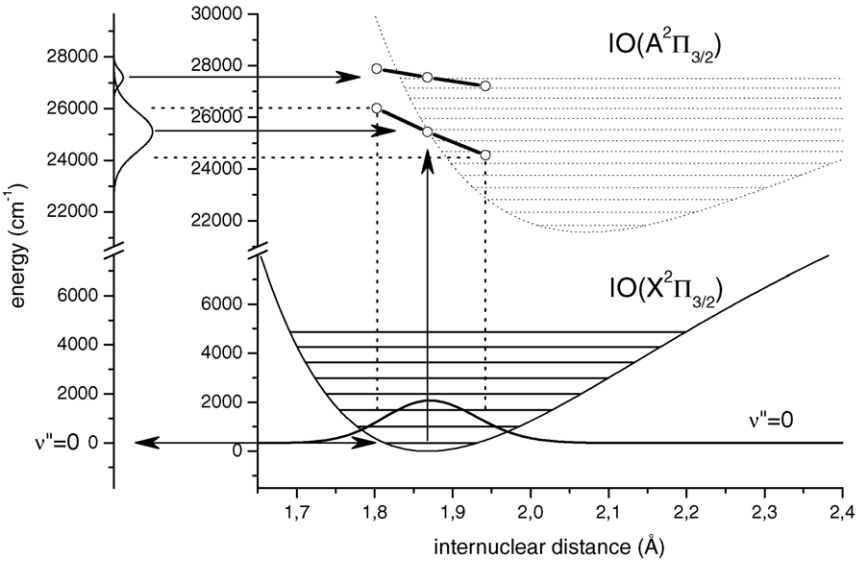

Fig. 12. By use of the reflection method two tangents to the hypothesised repulsive potentials were constructed (solid black lines, open circles). Their origin from the observed continua (left graph) and the state function at $\nu'' = 0$ (bottom) is indicated. Note the break of the vertical axis from 8000 to 21,000 cm^{-1}. The energy scale of the left graph has its origin in the $\nu'' = 0$ of $IO(X^2\Pi_{3/2})$.

repulsive potential. With the reflection method according to Condon (see e.g. [27,28]) it is furthermore possible to construct a tangent to the repulsive potential in that point, see Fig. 12. This approach assumes that the symmetric bell shaped ground state $\nu'' = 0$ state function can be graphically "reflected" at the repulsive potential to produce the observed bell shaped absorption continuum. A necessary pre-requisite to this is that curvature of the repulsive potential can be neglected. In that case the state functions obtained for the considered repulsive potential and determined at different energy levels do not differ much. Due to their maximum at the turning point and by consideration of the Franck–Condon principle this leads to effectively "sampling" the $\nu'' = 0$ state function as a function of internuclear distance r. Which can be approximated by the cited graphical reflection method. Note that in comparing the wavenumber axis of the spectrum to that of term energies, the energy of the lower level ($\nu'' = 0$) needs to be taken into account. The obtained coordinates for the tangents are listed in Table 1.

Considering the inclination of tangents and the atomic asymptote of possible dissociation products $I(^2P_{3/2}) + O(^3P)$ and $I(^2P_{1/2}) + O(^3P)$ enables a qualitative but plausible association of both, with the higher and less inclined one leading to $I(^2P_{1/2}) + O(^3P)$ and the other to $I(^2P_{3/2}) + O(^3P)$. In Fig. 13 an exponential decay was used to approximate this.

Intersection of the extrapolated lower repulsive potential in the middle of levels $\nu' = 2$ and $\nu' = 3$ seems to fit to the observed low predissociation of these levels. Newman et al. [14] proposed that the low predissociation of $\nu' = 2$ may be a fortuitous near cancellation of the overlap of bound and repulsive state wavefunctions at that energy. Level $\nu' = 1$ intersects near a turning point, where overlap of state functions will in any case be large leading to large predissociation, as observed in [14]. Levels with $\nu' > 3$ intersect closer to the inner turning points, where the state function has larger values and the overlap is also likely to be higher. The $\nu' = 0$ state does not intersect at all with the hypothetical repulsive potential, and consequently the overlap of state functions has to be small. This again is in agreement with the observations of [14], who report, that the $(0 \leftarrow 0)$ band shows small predissociation.

4.2. Origin of absorption continuum "X"

The continuum absorption "X" was extracted using the temporal behaviour of vibrationally excited $IO(\nu' \leftarrow \nu'')$, $\nu'' > 0$. But in spite of that the assignment of "X" to excited IO is not unequivocally, see above. Apart from the clear continuum "X" with maximum at about 27,700 cm^{-1} there is some weak evidence for a further smaller one below $(4 \leftarrow 1)$. Both were fitted by a gaussian, see Fig. 14 and then considered in the scheme of the reflection method, see Fig. 13. By starting from the continuum "X" as plotted on the energy scale on the left and considering reflection at any of the two repulsive potentials one ends at vibrational levels in the $IO(X^2\Pi_{3/2})$ which are high above the highest populated level $\nu'' = 7$. Assuming that transitions from $\nu'' > 0$ should dominantly couple to the same repulsive potentials as transitions from the ground state $\nu'' = 0$ it is obvious that "X"cannot have its origin in vibrationally excited $IO(X^2\Pi_{3/2}$, $\nu'' > 0)$.

An alternative plausible explanation of "X" is the sub-band system $A^2\Pi_{1/2} \leftarrow X^2\Pi_{1/2}$. According to ab initio work by Roszak et al. [29] the $A^2\Pi_{1/2}$ state does not form a potential well. In fact, they predicted a very difficult spectroscopic observation of this state due to its very strong predissociation. By reflecting the wave function of the vibrational ground state of $X^2\Pi_{1/2}$ into the $A^2\Pi_{1/2}$ potential calculated by [29], a featureless spectrum is obtained, which peaks near 27,000 cm^{-1}. Whether the $X^2\Pi_{1/2}$ could have been populated in our experiments or not can be checked to a first approximation by energy considerations. The

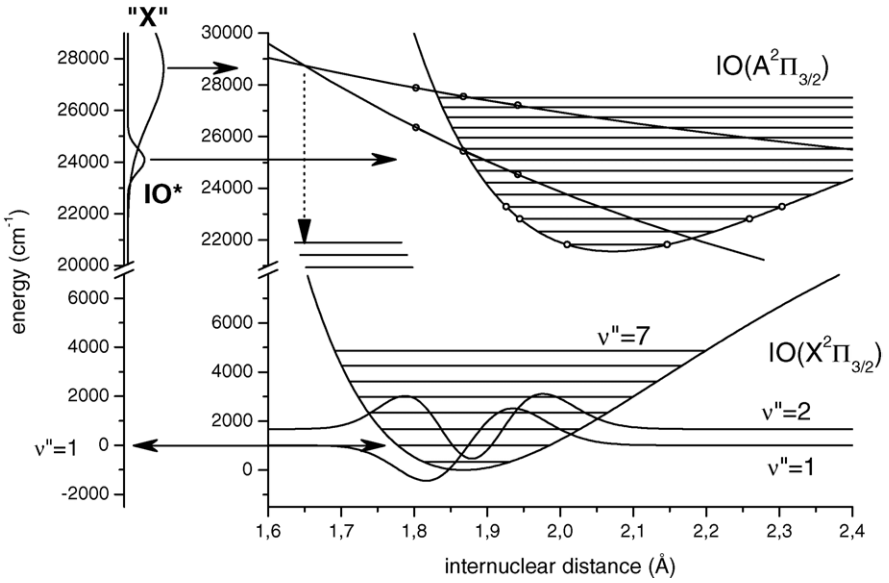

Fig. 13. The tangents constructed by the reflection method were extrapolated to plausible dissociation products. This extrapolation is based solely on geometric considerations and illustrates that the inclination of both tangents is plausible. The location of intersection of the lower repulsive potential with the different levels of the $A^2\Pi_{3/2}$ state fits to the observed pattern of predissociation reported by [14]. Applying the reflection method to the absorption "X" (upper left) proves that this cannot have its origin in vibrationally excited IO, as excitation of levels clearly above the last observed level $v'' = 7$ would be required. For the small continuum possibly present underneath IO^* no contradiction is encountered.

$X^2\Pi_{1/2}$, $v'' = 0$ state has an energy between that of $IO(X^2\Pi_{3/2})$, $v'' = 3$ and $v'' = 4$ [15]. On the other hand $IO(X^2\Pi_{3/2})$ of $v'' = 6$–7 were populated according to our observations. Therefore, in principle there was enough energy available to form $X^2\Pi_{1/2}$. Also its temporal behaviour being so similar to that of vibrationally excited IO $A^2\Pi_{3/2} \leftarrow X^2\Pi_{3/2}$, $v'' > 1$ makes a transition in the $^2\Pi_{1/2}$ system plausible. But the source of its formation needs to be clarified.

Other explanations for the observed absorption of "X" could assume that "X" is a different molecule. Having its origin only very shortly after the flash limits the available possibilities. IOO as a product of $I + O_2$ can be ruled out as in $I_2 + O_2$ flash photolysis experiments no evidence for a similar absorption was found. Reaction of $I + O_3 + M \rightarrow IO_3 + M$ with "X" being IO_3 could be a plausible alternative, especially as there is some correlation between the temporal behaviour of free iodine atoms observed by resonance absorption and the temporal behaviour obtained for "X". But the observed negative pressure dependence with "X" occurring dominantly at low pressure requires thermal dissociation of IO_3 to explain the observed behaviour in spite of the pressure-dependent formation.

For the small continuum, which is possibly present in the spectrum of vibrationally excited $IO(A^2\Pi_{3/2} \leftarrow X^2\Pi_{3/2}, v'' > 0)$ energies fit to bound-free transitions from $v'' = 1$ or 2 to the lower of the two repulsive states. Transitions to the upper one would fall into the flank of the larger observed continuum and would be covered by this. Their existence cannot be excluded.

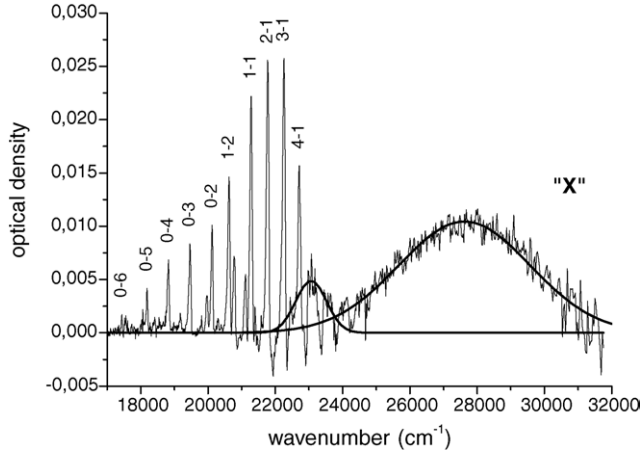

Fig. 14. In the spectrum extracted by usage of the temporal behaviour of vibrationally excited IO one strong continuum ("X") was found. Even though overlapped by artefacts from incomplete separation from ground state IO a second and smaller continuum could be inferred from the data, which according to Fig. 13 could be caused by vibrationally excited IO.

4.3. Determination of relative Franck–Condon factors for IO

Using the extracted spectra for ground state and excited states of IO relative band strengths were determined by integration of individual bands. Within each progression (common v'') all bands have the same temporal behaviour. Therefore the extraction of spectra from the overlapped time resolved data does not influence their relative band strength. Correct scaling of band strengths within one progression is preserved. But not between different progressions, because different progressions will in general have different temporal behaviour. As the spectrum for vibrationally excited IO was obtained for all $v'' > 0$ in one extraction and without discrimination between different v'', in the resulting spectrum the relative scaling *between* progressions is not preserved. Because of that, band strength obtained for bands of *different progressions* is not comparable.

Integrated optical density as a measure of band strength can be related to Franck–Condon factors (see [27]) and – by using the Franck–Condon principle – the dependence of the electronic transition moment $\mathbf{R}_{nm}$ on r can be neglected. By ignoring all other factors a proportionality between band strength and the squared overlap integral, i.e. the Franck–Condon factor for vibrational transition $n \rightarrow m$ is obtained:

$$\int_{\text{band}\,nm} A(\lambda) = \frac{8\pi^3 \nu_{nm}}{3hc} \cdot N_m \cdot \bar{\mathbf{R}}_{nm}^2 \cdot \left[\int_{r=0}^{\infty} \phi_n(r) \cdot \phi_m(r)\,\mathrm{d}r\right]^2 \propto \left[\int_{r=0}^{\infty} \phi_n(r) \cdot \phi_m(r)\,\mathrm{d}r\right]^2$$

As the scaling of band strengths between different progressions is not preserved by our extraction method, which produced the spectra, for each progression the relative band strengths within each band were scaled to the Franck–Condon factors published by Rao et al. [30]. Fig. 15 compares their values to those obtained from our measurements. Results for $\nu'' = 0$, $\nu' > 4$ are those obtained earlier from the constrained fit to the IO($\nu' \leftarrow 0$) continuum absorption. All others were obtained by direct integration of optical density across the band and subsequent scaling of the progression to the values by [30]. Also shown are the Franck–Condon factors obtained from our calculations based on a Morse potential approximation. In general the systematic behaviour of band strength obtained from our spectra is in good agreement with the ones predicted by [30]. Results are available as supplementary data alongside the electronic publication.

The results within the $\nu'' = 0$ progression agree well with both the results from [30] as well as those obtained using the Morse approximation for bands $\nu' < 4$ (scaling was performed for $\nu' = 3$). But for larger ν' – where no results by [30] exist – our estimates for Franck–Condon factors obtained from the constrained fit fall systematically below those from Morse approximation. This indicates some unresolved issues either in the constrained fit or in the Morse approximation. The former is quite likely, as the constrained fit is still prone to uncertainties. Also the estimated factors do not behave as smoothly as one would expect.

For $\nu'' = 1$ the agreement between all three series of Franck–Condon factors is strikingly good, while for larger ν'' – due to the smaller number of data points available – the agreement is less clear. But still the systematic pattern is followed closely by the estimates obtained from integrated bands. The magnitude of Franck–Condon factors of ($4 \leftarrow 0$) compared to ($2 \leftarrow 1$) and ($3 \leftarrow 1$) can also give a measure for the relative magnitude of absorption cross-section of these bands, because they all are outside of continuum regions and therefore have similar shape. This comparison indicates that the maximum cross-section in the $\nu'' = 1$ progression will be roughly 30% higher than that of the ($4 \leftarrow 0$) band, see [23].

4.4. Anomalous behaviour of IO($2 \leftarrow 0$)

4.4.1. Partial population inversion of IO($A^2\Pi_{3/2}$) at $\nu' = 2$ and $\nu' = 3$

The observed different temporal behaviour of the IO($2 \leftarrow 0$) and in parts also of the IO($3 \leftarrow 0$) can be explained in terms of a partial population inversion of these states. If a considerable number of IO molecules is formed in the IO($A^2\Pi_{3/2}$), $\nu' = 2$ and $\nu' = 3$ with sufficient life time, then stimulated emission could compete with absorption (thanks to one of the reviewers for helpful comment on this). The observed absorption in these bands would be weakened. This hypothesis is in line with the structure found for these bands in the CRDS measurements reported by Newman et al. [14]. Their measurements showed clear rotational structure and smallest predissociation for the ($2 \leftarrow 0$) transition and slightly larger for the ($3 \leftarrow 0$) transition. All other bands but the IO($0 \leftarrow 0$) are without rotational structure and are strongly predissociated. IO molecules formed in the $A^2\Pi_{3/2}$ state at $\nu' \neq 2$ and $\nu' \neq 3$ will therefore dissociate rather while molecules in $\nu' = 2$ and 3 have sufficient life time to undergo stimulated emission.

4.4.2. Possible source of IO in $A^2\Pi_{3/2}$ state

The comparison of temporal behaviour of IO($2 \leftarrow 0$) and the remaining IO($\nu' \leftarrow 0$) bands shows that the source of IO($A^2\Pi_{3/2}$) as the origin of the hypothesised partial population inversion is strongest during the initial period while towards the end both curves (after appropriate scaling) coincide accurately. Reversing the argument and subtracting the scaled IO($2 \leftarrow 0$) from the IO($4 \leftarrow 0$) produced a time curve which is a direct measure for the presence of IO undergoing stimulated emission from the $A^2\Pi_{3/2}$ state.

The lifetime of IO($A^2\Pi_{3/2}$), $\nu' = 2$ and $\nu' = 3$ with respect to radiative relaxation to the ground state and in the absence of stimulated emission is of the order of 10–100 ps, while the anomalous behaviour of IO($2 \leftarrow 0$) is observed over roughly 2.5 ms. This implies that a chemical source of IO($A^2\Pi_{3/2}$) must be present for the same order of time. Possible are both $O + I_2$ as well as $I + O_3$. Consideration of enthalpies of formation proves that only $O(^1D) + I_2$ is barely capable to form IO in the $A^2\Pi_{3/2}$ state, with the enthalpy of formation for IO according to Chase [31]. Strong chemiluminescence was directly observed by Miller and Cohen [15], which indicates significant population of the IO($A^2\Pi_{3/2}$) state. They used reaction $O + I_2$ at pressures at and below 1 mbar as source for IO and used the brightness of chemiluminescence as a diagnostic of successful IO production. In their experiment oxygen atoms were produced in an O_2 discharge. At the reported low pressures a large fraction of O atoms had to be expected in $O(^1D)$.

Opposed to these arguments is the short lifetime of $O(^1D)$ under the conditions of our experiments. Quenching of $O(^1D)$ with N_2 takes place at a rate of 2.6×10^{-11} cm^3 molecules^{-1} s^{-1} (and 4.05×10^{-11} cm^3 molecules^{-1} s^{-1} with O_2). At an overall pressure of 40 mbar concentrations of $[N_2]$ and $[O_2]$ were both of the order of 10^{17} molecules/cm^3. This gives $O(^1D)$ a lifetime of less than a microsecond. But according to the observation the source for IO($^2\Pi_{3/2}$) should be present over 2.5 ms. So even though a partial population inversion and stimulated emission could provide an explanation of the observed anomalous behaviour of the IO($2 \leftarrow 0$) transition, the source of IO($A^2\Pi_{3/2}$) remains unclear and requires further investigations.

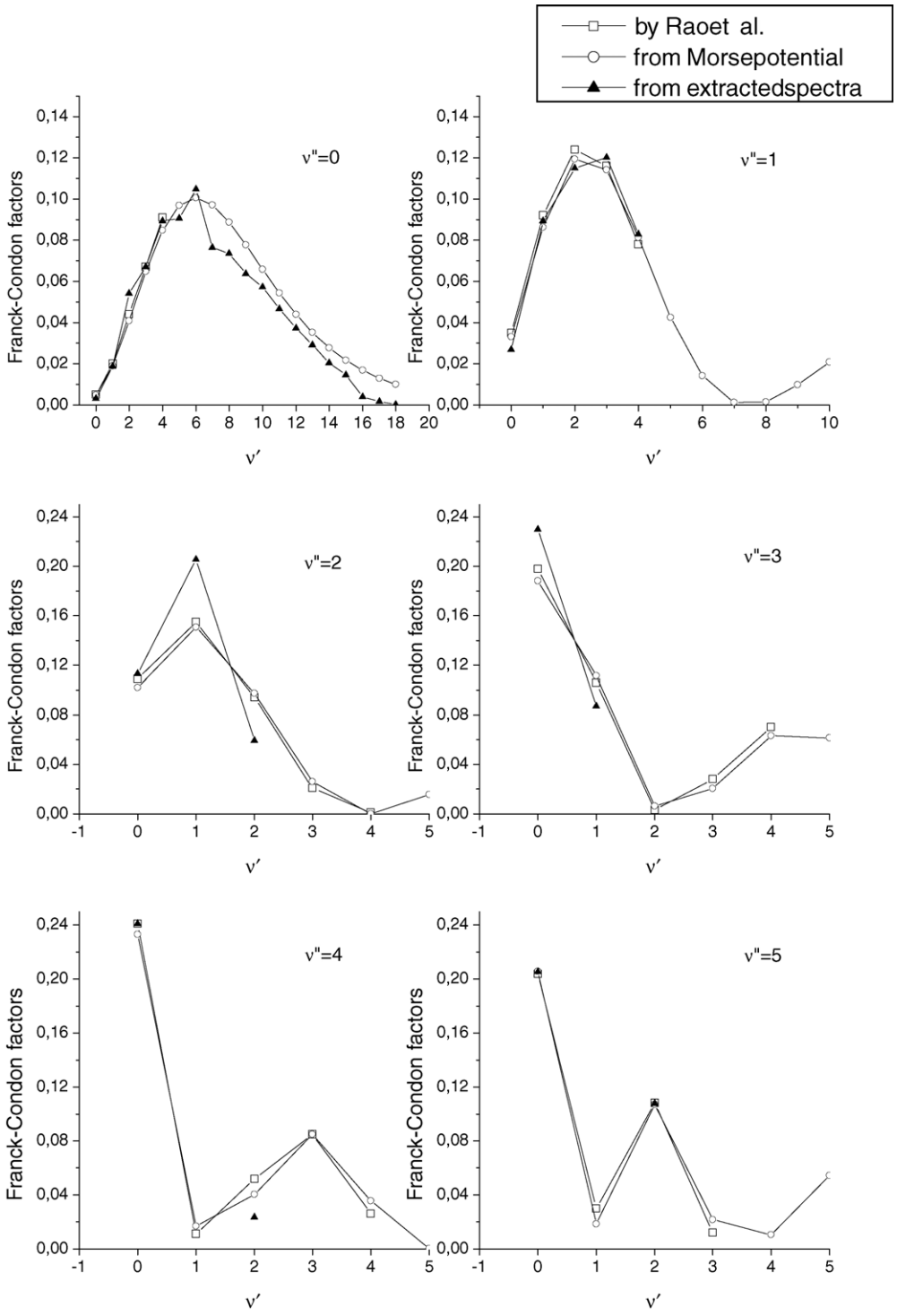

Fig. 15. In our spectra of ground state and excited IO band strength was estimated by integration across individual bands. After appropriate scaling they could be compared to Franck–Condon factors published by Rao et al. [30] as well as to those obtained in Morse approximation (see above). The agreement is good. For $\nu'' = 0$, $\nu' > 4$ inconsistencies remain between the results from a constrained fit and a Morse approximation.

5. Summary

Based on separation of absorber-specific temporal behaviour of optical density as obtained in the accompanying paper [23] and by use of multiple multivariate linear regression, spectra of iodine oxides formed in the photolysis of $I_2 + O_3$ have been obtained. For the first time overlapped spectra of ground state IO($\nu' \leftarrow 0$), vibrationally excited IO($\nu' \leftarrow \nu''$) with $\nu'' > 0$, and OIO could be separated from each other and from other underlying absorptions of other iodine oxides. The separated spectra could be shown to be free of other absorptions to better than ±3% [21]. The relative error of spectra in the regions with non-zero

absorption is of the order of 1–2% for the main absorbers IO and OIO as well as for the band peaks of vibrationally excited IO. For IO the critical issue of unidentified background absorption is thereby solved. Its continuum is well determined. Between the IO($4 \leftarrow 0$) and ($0 \leftarrow 0$) bands it was shown that absorption clearly returns to zero thereby removing the previously present uncertainty in differential absolute absorption cross-section. The same holds for the differential absorption cross-section of OIO. Even though our spectra have been recorded at low resolution of 1.3 nm FWHM only it was shown that in the previously published spectra systematic uncertainties dominate over resolution-dependent effects.

By the separation of the ground state IO spectrum from that of vibrationally excited IO the accuracy of spectroscopic measurements under non-equilibrium conditions is improved.

Three further absorber spectra labelled "X", "Y" and "Z" have been extracted from the data recorded in the 200–600 nm window. "Y" and "Z" are likely to being caused by I_2O_2 and I_2O_3, respectively [23] thereby providing part of the missing link between IO and OIO consumption and the formation of higher oxides and possibly aerosol. But a definite identification requires a careful study of the chemical mechanism, which is to be performed as the next step in this series of experiments. In any case the observed absorbers are part of the missing link between IO and OIO consumption and the formation of higher oxides and possibly aerosol. All spectra obtained in this work are available as supplementary data alongside the electronic version of this article as published in Elsevier Web Products.

Given the high quality of extracted spectra, for the first time an analysis of band strength of the IO($A^2\Pi_{3/2} \leftarrow X^2\Pi_{3/2}$) transition for ground state $\nu'' = 0$ and vibrationally excited IO with $\nu'' > 0$ was possible. The continuum absorption of the ground state IO spectrum could be resolved into overlapped bands of bound–bound transitions and two bound-free transitions. From the contribution of bound-free transitions to the observed absorption continuum the existence of two optically active repulsive states intersecting with the IO($A^2\Pi_{3/2}$) potential was inferred. By means of the reflection method tangents were determined to the two repulsive potentials. Correlating the tangents to probable dissociation products gave a plausible rough picture of the shape of the repulsive states. The resulting intersections with bound states within IO($A^2\Pi_{3/2}$) are in plausible agreement with observations on predissociation of states by [14] obtained by cavity ring down spectroscopy. Based on the repulsive states found it could be shown that the continuous absorption designated as "X" cannot be attributed to IO($A^2\Pi_{3/2}$, $\nu' \leftarrow X^2\Pi_{3/2}$, ν''), $\nu'' > 0$. But there is evidence that it could have its origin in the IO($^2\Pi_{1/2}$) sub-system. Relative band strength was determined for absorption bands originating from ground state and vibrationally excited states of IO($A^2\Pi_{3/2} \leftarrow X^2\Pi_{3/2}$). Comparison to Franck–Condon factors published by [30] as well as obtained from a Morse approximation shows a good agreement between the experimental values obtained from our spectra and the predicted ones. The anomalous behaviour of IO($2 \leftarrow 0$) was studied. It could be explained by a hypothetical partial population inversion and stimulated emission from IO($A^2\Pi_i$), but the source of the hypothesised inversion remains unclear.

Acknowledgements

This work was partially funded by the German Space Agency DLR through its support of the SCIAMACHY project and WTZ LVA 01/003, the European Union through contract EVK2-CT-2001-00104 THALOZ, and by the University and the State of Bremen. This work is part of and facilitated by IGBP-IGAC and EU-ACCENT Net work of Excellence.

Appendix A. Supplementary data

Supplementary data associated with this article can be found, in the online version, at doi:10.1016/j.jphotochem.2005.08.023.

References

[1] M.A.A. Clyne, H.W. Cruse, Trans. Faraday Soc. 66 (1970) 2227–2236.
[2] R.A. Cox, G.B. Coker, J. Phys. Chem. 87 (1983) 4478–4484.
[3] R.E. Stickel, A.J. Hynes, J.D. Bradshaw, W.L. Chameides, D.D. Davies, J. Phys. Chem. 92 (1988) 1862–1864.
[4] A.A. Turnipseed, M.K. Gilles, J.B. Burkholder, A.R. Ravishankara, Chem. Phys. Lett. 242 (1995) 427–434.
[5] B. Laszlo, M.J. Kurylo, R.E. Huie, J. Phys. Chem. 99 (1995) 11701–11707.
[6] M. Harwood, J. Burkholder, M. Hunter, R. Fox, A. Ravishankara, J. Phys. Chem. A 101 (1997) 853–863.
[7] D.B. Atkinson, J.W. Hudgens, A.J. Orr-Ewing, J. Phys. Chem. A 103 (1999) 6173–6180.
[8] T. Ingham, M. Cameron, J.N. Crowley, J. Phys. Chem. A 104 (2000) 8001–8010.
[9] J.W. Bloss, D.M. Rowley, R.A. Cox, R.J. Jones, J. Phys. Chem. 105 (2001) 7840–7854.
[10] R.A. Durie, D.A. Ramsay, Can. J. Phys. 36 (1958) 35–53.
[11] R.A. Durie, F. Legay, D.A. Ramsay, Can. J. Phys. 38 (1960) 444–452.
[12] S. Himmelmann, J. Orphal, H. Bovensmann, A. Richter, A. Ladstaetter-Weissenmayer, J.P. Burrows, Chem. Phys. Lett. 251 (1996) 330–334.
[14] S.M. Newman, W.H. Howie, I.C. Lane, M.R. Upson, A.J. Orr-Ewing, J. Chem. Soc., Faraday Trans. 94 (1998) 2681–2688.
[15] C.E. Miller, E.A. Cohen, J. Chem. Phys. 115 (14) (2001) 6459–6470.
[16] S.H. Ashworth, B.J. Allan, J.M.C. Plane, Geophys. Res. Lett. 29 (2002) 65-1–65-4, doi:10.1029/2001GL13851.
[17] C.E. Miller, E.A. Cohen, J. Chem. Phys. 118 (10) (2003), doi:10.1063/1.1540107.
[18] S.P. Sander, J. Phys. Chem. 90 (1986) 2194–2199.
[19] S. Solomon, A.L. Schmeltekopf, W.R. Sanders, J. Geophys. Res. 92 (1987) 8311–8319.
[20] U. Platt, Air Monitoring by Spectroscopic Techniques, Chemical Analysis Series 127, Wiley, New York, 1994 (Chapter 2).
[21] J.C. Gómez Martín, P. Spietz, J. Orphal, J.P. Burrows, Spectrochim. Acta A 60 (2004) 2673–2693.
[22] P. Spietz, Absorption cross sections for iodine species of relevance to the photolysis of mixtures of I_2 and O_3 and for the atmosphere, Thesis submitted within the doctoral program "Dr. rer. nat.", Department of Physics, University of Bremen, 2005.
[23] J.C. Gómez Martín, P. Spietz, J.P. Burrows, J. Photochem. Photobiol. A, 2005, this issue.
[24] A. Dahlquist, A. Björk, N. Anderson, Numerical Methods, Prentice-Hall, Englewood cliffs, NJ, 1974.

[25] P. Spietz, J.C. Gómez Martín, J.P. Burrows, Spectrochim. Acta Part A: Mol. Biomol. Spectrosc., in press.
[26] P.M. Morse, Phys. Rev. 34 (1929) 57–64.
[27] G. Herzberg, Molecular Spectra and Molecular Structure, I. Spectra of Diatomic Molecules, Krieger Publishing Company, Malabar, FL, 1950.
[28] P. Sulzer, K. Wieland, Helv. Phys. Acta 25 (1952) 653–676.
[29] S. Roszak, M. Krauss, A.B. Alekseyev, H.-P. Liebermann, R.J. Buenker, J. Phys. Chem. A 104 (2000) 2999–3003.
[30] M.L.P. Rao, D.V.K. Rao, P.T. Rao, Phys. Lett. 50A (5) (1974) 341–342.
[31] M.W. Chase Jr., J. Phys. Chem. Ref. Data 25 (5) (1996) 1297–1339.